Organic Acid-Catalyzed Polyurethane Formation via a Dual-Activated Mechanism: Unexpected Preference of N-Activation over O-Activation of Isocyanates

Haritz Sardon,*,[†,‡] Amanda C. Engler,[†] Julian M. W. Chan,[†] Jeannette M. García,[†] Daniel J. Coady,[†] Ana Pascual,[†,‡] David Mecerreyes,[‡,§] Gavin O. Jones,[†] Julia E. Rice,[†] Hans W. Horn,*,[†] and James L. Hedrick*,[†]

[†]IBM Almaden Research Center, 650 Harry Road, San Jose, California 95120, United States

[‡]POLYMAT, University of the Basque Country UPV/EHU Joxe Mari Korta Center, Avda. Tolosa 72, 20018 Donostia-San Sebastián, Spain

[§]Ikerbasque, Basque Foundation for Science, Alameda Urquijo 36-5 Plaza Bizkaia, 48011 Bilbao, Spain

S *Supporting Information*

ABSTRACT: A systematic study of acid organocatalysts for the polyaddition of poly(ethylene glycol) to hexamethylene diisocyanate in solution has been performed. Among organic acids evaluated, sulfonic acids were found the most effective for urethane formations even when compared with conventional tin-based catalysts (dibutyltin dilaurate) or 1,8-diazabicyclo[5.4.0]undec-7-ene. In comparison, phosphonic and carboxylic acids showed considerably lower catalytic activities. Furthermore, sulfonic acids gave polyurethanes with higher molecular weights than was observed using traditional catalyst systems. Molecular modeling was conducted to provide mechanistic insight and supported a dual activation mechanism, whereby ternary adducts form in the presence of acid and engender both electrophilic isocyanate activation and nucleophilic alcohol activation through hydrogen bonding. Such a mechanism suggests catalytic activity is a function of not only acid strength but also inherent conjugate base electron density.
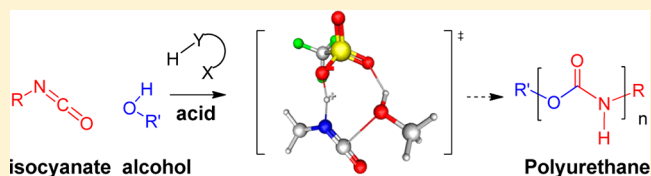
INTRODUCTION

Polyurethanes (PUs) constitute one of the most important classes of polymeric materials with applications ranging from high-performance structural applications to foam padding.[1] Due to their extreme utility and relatively low cost, these materials account for nearly 5 wt % of total worldwide polymer production and are expected to exceed 18 kilotons annually by 2016. Additionally, PU material properties are easily tailored through structural variation of the monomers.[2,3] As a result, they function in a wide variety of processing methods giving rise to surface coatings, foams, and dispersions.[4−6] PUs are primarily synthesized by two routes:[7] (1) reaction of diisocyanates with diols and (2) reaction of bis-carbonates with diamines at low temperatures.[8,9] The former reaction is preferred because of its atom economy, though a catalyst is generally required.[1,10] Organotin compounds have predominantly filled this catalytic role; however, their removal from PUs is often exceedingly difficult, resulting in deterious residual catalyst being left behind.[7,11] Several attempts have been made to replace tin with more environmentally benign organometallic catalysts featuring bismuth, aluminum, or zirconium.[12−14] However, reaction rates and molecular weights achieved using these catalysts have not produced efficiencies warranting organotin replacement.[15]

Traditional organometallic catalysts,[16] organic bases,[17−20] N-heterocyclic carbenes (NHCs),[21] and organic acids[11,22] have all been shown to efficiently catalyze controlled ring-opening polymerization (ROP) of lactones, ethers, esters, and carbonates.[23−26] In the case of PUs, organometallic catalysts and organic bases have largely dominated the field.[15,27] Recently, Cramail et al.[15] demonstrated a highly efficient alcohol/isocyanate polymerization catalyzed by bicyclic penta-alkylated guanidine. Using this catalyst they reported PUs with molecular weight values comparable to tin catalysis.[15] A similar organocatalyst, 1,8-diazabicyclo[5.4.0]undec-7-ene (DBU), achieved molecular weights (M_w) up to 74 000 Da when polymerizing isophorone diisocyanate (IPDI) with PTMO-650 at 60 °C.[15] Unfortunately, polymerization rates of nucleophilic activating organocatalysts are generally slow and require heat for high conversions.[15,28]

Besides the organic bases, organic acids have also been shown to be effective catalysts for the ROP of ε-caprolactone and δ-valerolactone.[29] More recently, efficient polymerizations of cyclic carbonates have also been reported,[10,30] and density functional theory (DFT) calculations and detailed kinetic analysis pointed towards a dual-activation mechanism, whereby

the monomer carbonyl and the propagating hydroxy group underwent concurrent hydrogen-bonding activation. As a consequence, both the acid and its conjugate base played an important role in catalysis.

There have been very few studies utilizing organic acids in PU polymerizations, and their results have generally been inferior to those achieved by metallic catalysts. Yezrielev et al.[31] showed dinonylnaphthalenedisulfonic acid effectively catalyzed polyaddition of phenolic ester alcohols with aliphatic isocyanates; however, molecular weights were not reported. Nordstrom et al.[32] reported an organic acid-catalyzed reaction between isocyanates and alcohols at high temperatures, but their results were less favorable than tin-catalyzed polymerizations.

Herein, a systematic investigation into acid-catalyzed polyaddition of diols with aliphatic diisocyanates affording high M_w is disclosed. Furthermore, using DFT calculations performed on model systems, a dual-activation mechanism is believed to be operative.

■ RESULTS AND DISCUSSION

Acid-Catalyzed PU Formation. Acid-catalyzed polymerization studies were performed using a model reaction of hexamethylene diisocyanate (HDI) and poly(ethylene glycol) (M_n =1500 Da (PEG$_{1500}$) (Scheme 1a). This system was

Scheme 1. (a) Organic Acid-Catalyzed Synthesis of PUs from Hexamethylene Diisocyanate and PEG$_{1500}$ Diol and (b) Acid Catalysts Employed in the Screening Process
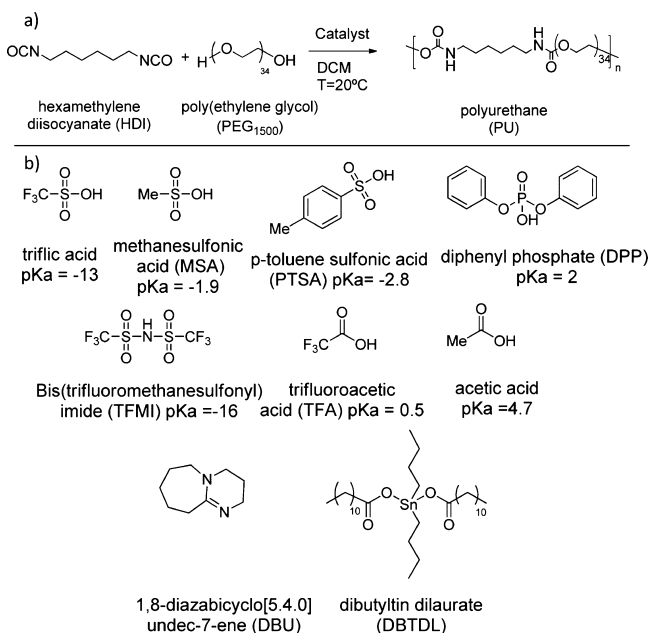
selected because its commercial availability and convenient monitoring handles (^{1}H NMR). Commercial organic acid catalysts of varied functionality and pK_a were evaluated for PU synthesis and compared to commonly used DBU and DBTDL (Scheme 1b).

Polymerization studies were accomplished by dissolving equimolar amounts of HDI and PEG$_{1500}$ in dichloromethane (0.1 M) followed by addition of catalyst (5 mol %). Using ^{1}H NMR, the polymerizations were monitored by a diagnostic disappearance of HDI methylene protons (δ 3.32 ppm, adjacent to the isocyanate) and their subsequent reappearance

at δ 3.15 ppm. Monomer conversion was determined using relative peak integrations values (Supporting Information). Table 1 lists molecular weight and polydispersities (PDI) for

Table 1. Conversion Rate and Molecular Weight Distribution for Different Catalysts[a]

acid	conv (%) 6h[b]	M_w kDa	PDI	time to >98% conv (h)	M_w kDa	PDI
none	<2	1.9	1.1	NA	2.0	1.1
DBU	86	9.2	1.7	24	22.0	1.4
DBTDL	82	7.4	1.7	24	24.0	1.4
TFMI	≥98	24.8	1.4	6	29.8	1.5
triflic acid	≥98	23.5	1.3	6	28.2	1.5
PTSA	97	18.5	1.9	8	23.6	1.7
MSA	88	10.1	1.7	24	18.3	1.3
TFA	3	2.0	1.1	N/A	2.0	1.2
DPP	50	4.3	1.4	48	23.7	1.7
acetic acid	2	2.0	1.1	N/A	2.0	1.1

[a]At 6 h using a ratio of PEG$_{1500}$/HDI/catalyst of 1/1/0.05 in dichloromethane (DCM, 0.1 M with respect to monomer) at 20 °C. [b]Conversion = peak integration of the methylene protons adjacent to the isocyanate/urethane linkage × 100%.

each polymerization using the various acids. For comparative purposes DBU and DBTDL were also included as polymerization controls along with an uncatalyzed reaction.

The rate of polymerization and molecular weight were found to be highly catalyst dependent. Without a catalyst, monomer conversion was negligible after 6 h, and full conversion was not achieved. Conversely, the sulfonic acids were extremely active, as observed by triflic acid and TFMI exhibiting conversions exceeding 98%. This was a very favorable result compared to the conversions obtained from DBTDL and DBU (82% and 86%, respectively) after 6 h. Diphenylphosphate (DPP), a relatively weak acid, catalyzed PU polymerization (50% conversion in 6 h), however, 48 h was required to obtain full conversion. Carboxylic acids (TFA and acetic acid) were found ineffective and gave conversions of 3% or less at 6 h. However, when stoichiometric amounts were applied complete monomer conversions were seen after 48 h, albeit with reduced molecular weights. GPC analysis of sulfonic acid-catalyzed PUs showed considerably higher molecular weights than DBU or DBTDL catalyzed reactions. PDI ranged from 1.3 to 1.7 for all catalyst tested. Moreover, none of the PU degradation normally seen with DBU and DBTDL was observed after one week in the presence of acid catalyst (see Supporting Information for details).

To more precisely compare catalytic activities, kinetic studies for each catalyst were performed. The reaction proceeded with overall third-order kinetics $-d[M]/dt = k[acid][M]^2$, (where $[M]$ = $[diol]$ = $[diisocyanate]$) as confirmed by the linear relationship between time, t and $1/(1 - p)$ where p is the fraction of monomer converted to polymer.[33] Apparent rate constants, k' were obtained for each polymer, where k' = $k[acid]$ (Figure 1). The reaction was found to be first order with respect to acid concentration (Supporting Information).

The results in Table 1 showed a loose inverse correlation between pK_a and catalytic activity: lower pK_a produced larger rate constant. However, since carboxylic acids provided minimal catalytic activity, a more comprehensive explanation was required. To further probe the reaction kinetics, a parallel experiment was carried out using 1-hexanol and resulted in
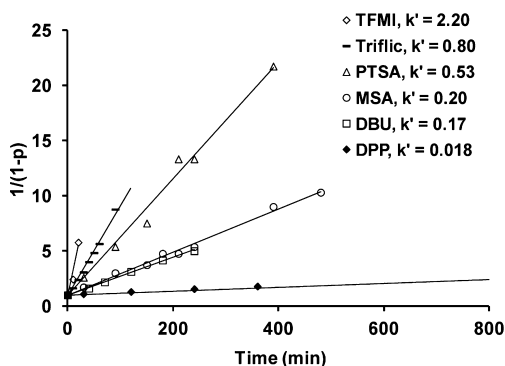
Figure 1. Linear plot of $1/(1 - p)$ as a function of time for the acid-catalyzed polymerization. $k' = k[\text{acid}]$ (units of M^{-1} s^{-1}) was determined from the slope.

analogous kinetics as found with PEG_{1500} diol (see Supporting Information) suggesting that urethane formation follows the same trend as polyurethane formation, allowing the simplification of the computational modeling.

Computational Modeling. A comprehensive computational study was conducted with GAMESS-US[34] using M11 DFT[35] to determine possible mechanistic pathways of different acids (triflic acid, MSA, dimethyl phosphate (DMP, pK_a =1.3, as a model for DPP) and acetic acid) as well as the basic catalyst DBU.[36−38] To make the computational study tractable, a simple isocyanate and alcohol were selected for the model reaction (Figure 2).

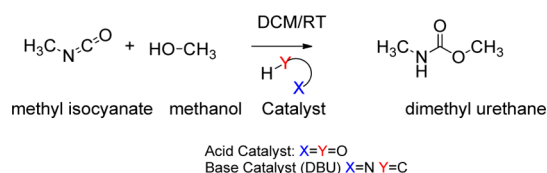Acid Catalyst: X=Y=O
Base Catalyst (DBU) X=N Y=C

Figure 2. An acid-catalyzed reaction between an isocyanate and an alcohol to give a urethane.

The significance of dual activation by certain acid catalysts in the ROP of cyclic esters and carbonates has been recognized recently.[11,29] It was envisaged that a similar pathway may also be operative during urethane formation. However, unlike with ROP, electrophilic activation can occur at two locations: isocyanate activation via hydrogen bonding to the O atom (Figure 3a) or to the N atom (Figure 3b). Nucleophilic activation of the alcohol via hydrogen bonding between the acid and the hydroxyl H ($O-H\cdots X$) (Figure 3c) was analogous to our previous ROP report. In the case of basic catalysis by
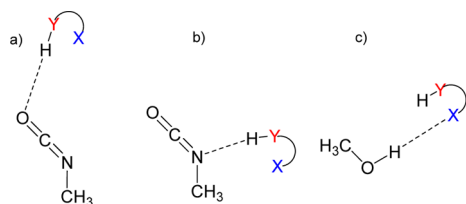

Figure 3. Binary adducts of acids or bases with methyl isocyanate (CH_3NCO) or with methanol (CH_3OH); electrophilic activation of isocyanate via: (a) O and (b) N atoms and (c) nucleophilic activation of the alcohol.

DBU, nucleophilic activation of the alcohol initiator is the only mode of activation that is operative.

Binary Adducts. The catalysts were characterized in terms of their adducts with methyl isocyanate as well as with methanol by separately examining the electrophilic and nucleophilic activation. Since two types of binary hydrogen-bonded adducts between the acid (A−OH) and the isocyanate are conceivable (Figure 3a,b), binding free energies for adduct formation (Table 2) were used to determine most probable

Table 2. Binding Free Energies of Binary Hydrogen-Bonded Adducts between an Acid Catalyst and Methyl Isocyanate in Which the Catalyst Serves As Hydrogen-Bond Donor and Acid or Base Catalyst and Methanol in Which the Catalyst Serves As Hydrogen-Bond Acceptor[a]

	binding free energy [kcal/mol] to methyl isocyanate			binding free energy [kcal/mol] to methanol
	O-bound	N-bound		
acid/base catalyst	covalent	covalent	ion pair	covalent
triflic acid	−9.7	−8.1	−5.3	−2.3
MSA	−8.0	−5.8	N/A	−3.0
DMP	−7.9	−5.7	N/A	−6.1
acetic acid	−6.1	−3.7	N/A	−4.5
DBU	N/A	N/A	N/A	−8.3

[a]Optimized 3D structures are shown in Supporting Information.

adduct structures. Notably, the bent conformation of methyl isocyanate becomes linear upon triflic acid hydrogen bonding to the O atom of the isocyanate (Supporting Information). Moreover, it was observed that binding energies for formation of O-bound adduct decreases as the pK_a of the acid decreases (Table 2). This was also true for the N-bound hydrogen-bonded adducts. Overall, calculations predict that O-bound hydrogen-bonded adducts are more stable than N-bound hydrogen-bonded adducts with triflic acid being the most powerful hydrogen-bond donor (i.e., electrophilic activator). These results are consistent with other recent findings showing that tin-based catalysts activate by binding to the oxygen atom of the isocyanate.[39]

Binary adducts of acid/base catalysts with methanol in which the catalyst accepts a hydrogen bond from the alcohol (Figure 3c) can serve as probe into the extent of nucleophilic activation by the catalyst (Table 2). Here it is seen that DMP is the best hydrogen-bond acceptor (i.e., nucleophilic activator) among the acids studied (only surpassed by basic DBU), while nucleophilic activation by triflic acid is practically nonexistent.

Non-Activating Ternary Adducts. Ternary hydrogen-bonded adducts formed between an acid catalyst, methanol, and methyl isocyanate were found computationally (Figure 4) in which the alcohol donates a hydrogen bond to the O atom (Figure 4a, "O-bound") or N atom (Figure 4b, "N-bound") belonging to isocyanate while accepting a hydrogen bond from the acid. Of note is that these ternary adducts are activating neither the isocyanate nor the alcohol. As shown in Table 3 these non-activating ternary adducts are stronger bound than their dual-activated counter parts (RC, Supporting Information) suggesting that the former will play a vital role in the pathway of the urethane formation reaction catalyzed by acids
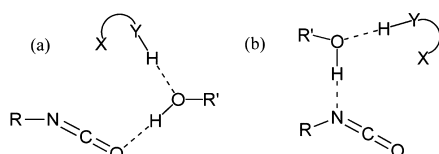
Figure 4. Possible non-activating ternary hydrogen-bonded adducts between an acid catalyst, methanol, and methyl isocyanate: (a) O-bound and (b) N-bound. The ternary species depicted here are labeled "Adduct" in the reaction profiles shown in Figure 6.

Table 3. Binding Free Energies of Non-Activating Ternary Hydrogen-Bonded Adducts between an Acid Catalyst, Methanol, and Methyl Isocyanate

	binding free energy of non-activating ternary adducts [kcal/mol]	
acid catalyst	O-bound	N-bound
triflic acid	−23.5	−21.6
MSA	−17.4	−15.9
DMP	−17.6	−14.4
acetic acid	−13.2	−12.2

(optimized 3D geometries are shown in Supporting Information).

Dual-Activated Mechanisms of Urethane Formation: Unexpected Preference of N-Activated over O-Activated pathway. General mechanisms for the acid-catalyzed O-activated and N-activated formation of urethane from isocyanate and alcohol have been proposed in Figure 5. Note
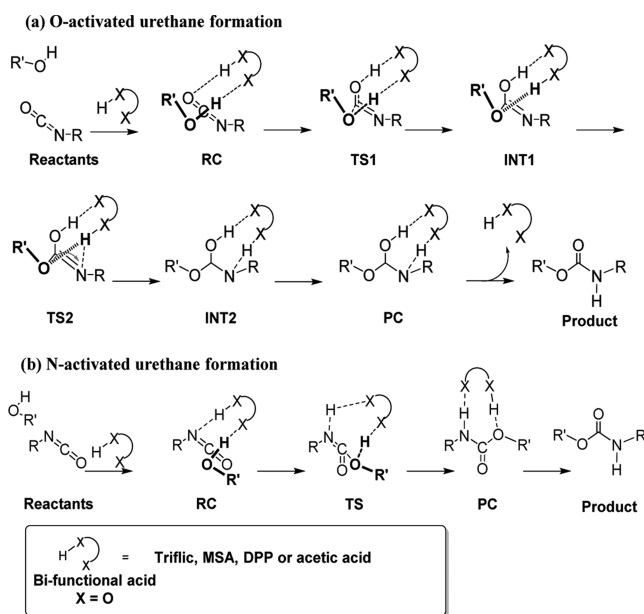

Figure 5. Idealized mechanism for the (a) O-activated and (b) N-activated acid-catalyzed urethane formation from isocyanate and alcohol.

that at any stage of the pathway the acid catalyst maintains two hydrogen bonds with the reagents or any reactive species along the pathway. The initial step in these mechanisms involves the formation of reactant complexes (RC) in which the acid catalyst, the alcohol, and the isocyanate are bound to each other by weak intermolecular interactions such as hydrogen bonding and dispersion forces (Supporting Information). Several

plausible pathways of acid-catalyzed urethane formation (consistent with Figure 5) were examined. Only the ones that lead to the thermodynamic product dimethyl urethane with an E-amide and a Z-ester conformation (Supporting Information) are reported.

O-Activated Urethane Formation. Figure 6a depicts reaction profiles for the acid-catalyzed O-activated formation of dimethyl urethane using acid catalysts as well as using DBU as base catalyst (no N- or O-activation possible in this case). The barriers for the initial step ("TS1") as listed in Table 4 are inconsistent with experimentally observed catalytic activities (Table 1).

N-Activated Urethane Formation. Figure 6b depicts reaction profiles for the acid-catalyzed N-activated formation of dimethyl urethane using acid catalysts as well as base-catalyzed urethane formation by DBU. Table 4 shows rate-limiting barriers for these processes. Surprisingly, the rate-limiting barriers for acid-catalyzed N-activation are significantly lower than the corresponding barriers for O-activation, and unlike the latter are consistent with experimental results showing an inverse correlation between the pK_as of the organic acids and their catalytic activities (Table 1).

The exception is DBU: experimentally DBU is as fast as MSA and much faster than DMP and acetic acid (Figure 1), but computationally DBU is predicted to be marginally slower than all acids except for acetic acid. This is probably due to the propensity of acids to dimerize and thus reduce their effective concentrations; this has not been captured by our calculations.[11] Of course, DBU does not dimerize as these acids do. Finally, the surprisingly high activity of DMP despite its weak acidity can be attributed to its strong ability to nucleophilically activate the alcohol (see Table 2b).

Close inspection of the TS geometry for the reaction catalyzed by triflic acid (Figure 7a) reveals that the protonation of the N atom is the actual transition mode, while the formation of the C−O bond between the isocyanate and the alcohol occurs later. This was confirmed via an intrinsic reaction coordinate (IRC) calculation. In contrast, the TS geometry for the profile with DMP (Figure 7b) shows that the C−O bond between the isocyanate and the alcohol forms first. An IRC calculation indicated subsequent protonation of the N atom of the isocyanate, followed by proton transfer from the alcohol to DMP.

Finally, in the case of MSA both processes occur simultaneously due to the moderate acidity of MSA. These findings are presented in the Supporting Information that accompanies this article.

Ability to Polymerize IPDI, a Low-Reactivity Isocyanate, Using Organic Acids. IPDI is one of the most widely used monomers for PU formation. Despite being a cyclo-aliphatic isocyanate, IPDI polymers exhibit good oxidative, ultraviolet, and thermal stabilities. However, it has considerably lower reactivity when compared to HDI because it possesses a secondary isocyanate.[12] Generally, this fact is circumvented through harsh polymerization conditions or large catalyst loadings to obtain high molecular weights.[15]

In order to demonstrate acid catalysis efficiency for polymerizing less reactive isocyanates, IPDI was polymerized with poly(ethylene glycol) (M_n =1500 Da (PEG$_{1500}$) using triflic acid at ambient temperature (Scheme 2). The diagnostic isocyanate stretching frequency (2270 cm^{-1}) was completely converted to new urethane signals as evidenced by the
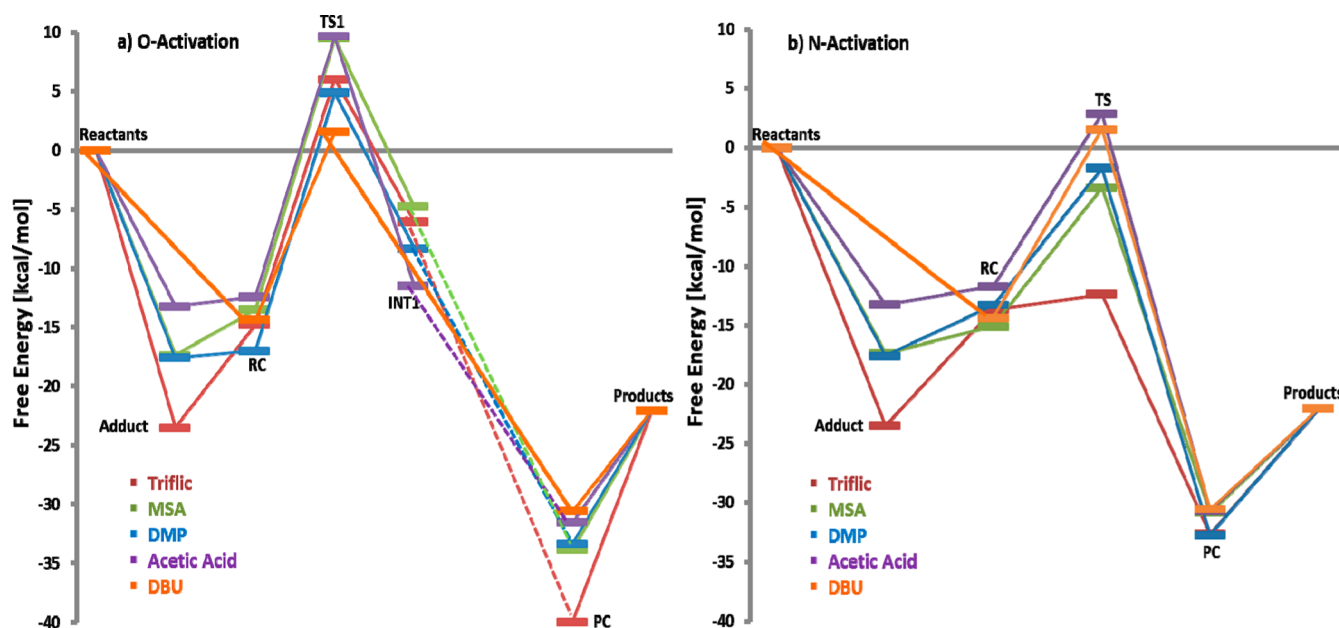
Figure 6. Reaction profiles for the acid-catalyzed (a) O-activated formation and (b) N-activated formation of dimethyl urethane from methyl isocyanate and methanol using triflic acid, MSA, DMP, and acetic acid as acid catalysts. The species labeled "Adduct" do not lie on the actual pathway but are the ones with the lowest free energy, the O-bound non-activating ternary acid-CH_3OH-CH_3NCO adducts (see Figure 4b and Supporting Information).

Table 4. Free Energy of Activation $\Delta G^{\ddagger}$ [kcal/mol] for O-Activated and N-Activated Acid/Base-Catalyzed Urethane Formation Evaluated with Respect to the O-Bound Non-Activating Ternary Acid-CH_3OH-CH_3NCO Adducts

	free energy of activation $\Delta G^{\ddagger}$ [kcal/mol]	
acid/base catalyst	O-activated	N-activated
triflic acid	29.5	11.1
MSA	25.4	14.0
DMP	22.0	14.8
acetic acid	22.8	16.1
DBU		15.9

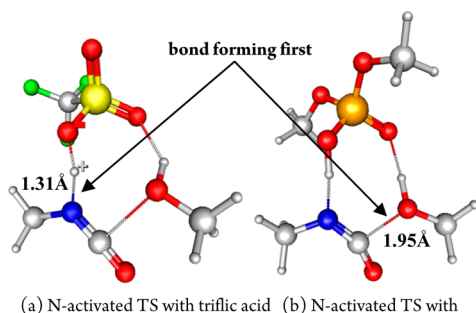(a) N-activated TS with triflic acid (b) N-activated TS with

Figure 7. Transition-state geometries for the acid-catalyzed N-activated formation of dimethyl urethane from methyl isocyanate and methanol using (a) triflic acid and (b) DMP as acid catalysts.

Scheme 2. PU Synthesis from IPDI and PEG$_{1500}$ Diol in the Presence of Triflic Acid

isophorone diisocyanate (IPDI)   poly(ethylene glycol) (PEG)   polyurethane (PU)
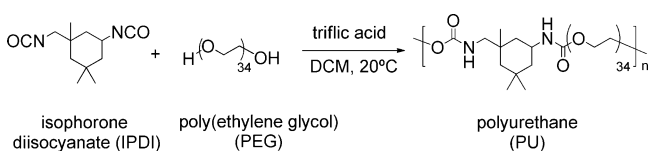
appearance of two new carbonyl stretching signals at 1570 and 1720 cm^{-1} (Figure 8) after only 6 h.
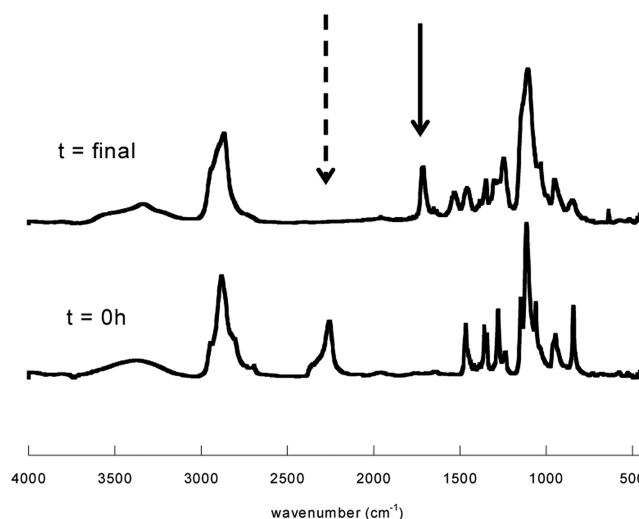

Figure 8. Infrared spectra recorded at $t = 0$ and at >98% conversion in the presence of triflic acid.

This was an import observation as it highlights the asymmetry of IPDI wherein it forms two nondegenerate urethanes linkages. Polymer formation was further confirmed using GPC analysis (Supporting Information). The newly formed IPDI PU possessed a M_w of 30.1 kDa and a PDI of 1.35 (Supporting Information ^{1}H NMR and GPC of the synthesized system).

Solvent-Free Synthesis of Polyurethanes Using Organic Acids. Polyurethanes are generally synthesized using an organic solvent. However, environmental concerns have led researchers to look for greener technologies which can reduce waste stream efflux.[40]

Continuing this trend, organic acids were evaluated under bulk polymerization conditions. The solventless polymerization of HDI and poly(propylene glycol) (M_n =1000 Da (PPG_{1000}) in the presence of triflic acid at 60 °C (Scheme 3) produced 35.3 kDa polymer as shown by GPC (Figure 9), regardless of PPG having less reactive secondary alcohols.

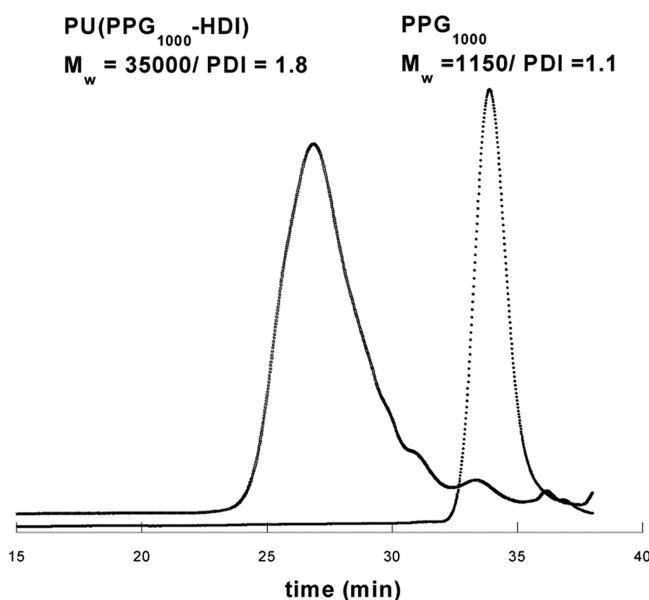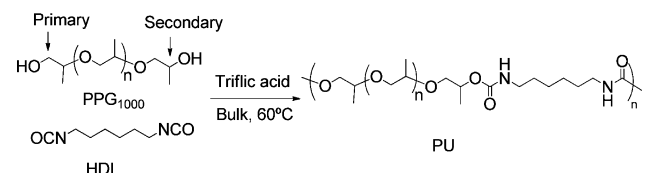**Scheme 3. PU Synthesis from HDI and PPG_{1000} Diol in the Presence of Triflic Acid**

Figure 9. GPC traces of starting material (PPG_{1000}) and resulting polyurethane PU(PPG_{1000}-HDI) near full conversion.

CONCLUSIONS

In conclusion, the ability to synthesize polyurethanes from diisocyanates and diols using organic acid catalysts has been demonstrated. Sulfonic acids were found to activate isocyanates more efficiently than tin-based catalysts while also producing a higher molecular weight polymer. DFT calculations indicated that the reaction followed a dual hydrogen-bonding mechanism involving electrophilic activation of the isocyanate via the isocyanate nitrogen, with simultaneous nucleophilic activation of the alcohol. This suggests that the strength of a given acid as well as the nucleophilicity of its conjugate base play vital roles in catalyzing urethane formation. Calculations also predicted that, unexpectedly, non-activating ternary adducts between isocyanate, acid, and alcohol were found computationally that are significantly lower in free energy than their dual-activated counter parts. The use of acid catalysis is expected to greatly expand the scope of metal-free polyurethane syntheses under both solution and bulk polymerization conditions, especially when considering its efficacy for polymerizing sterically hindered secondary alcohols and isocyanates.

ASSOCIATED CONTENT

Ⓢ Supporting Information

Details of molecular modeling experiments, GPC data, and ^{1}H NMR spectra. This material is available free of charge via the Internet at http://pubs.acs.org.

AUTHOR INFORMATION

Corresponding Authors

haritz.sardon@ehu.es
hedrick@us.ibm.com
hanshorn@us.ibm.com

Notes

The authors declare no competing financial interest.

ACKNOWLEDGMENTS

REFERENCES

(1) Chattopadhyay, D. K.; Raju, K. V. S. N. *Prog. Polym. Sci.* **2007**, *32*, 352−418.
(2) Cherng, J. Y.; Hou, T. Y.; Shih, M. F.; Talsma, H.; Hennink, W. E. *Int. J. Pharm.* **2013**, *450*, 145−162.
(3) Engels, H.-W.; Pirkl, H.-G.; Albers, R.; Albach, R. W.; Krause, J.; Hoffmann, A.; Casselmann, H.; Dormish, J. *Angew. Chem., Int. Ed.* **2013**, *52*, 9422−9441.
(4) Chattopadhyay, D. K.; Webster, D. C. *Prog. Polym. Sci.* **2009**, *34*, 1068−1133.
(5) Hepburn, C. *Polyurethane elastomers*; 2nd ed.; Elsevier Applied Science: New York, 1992.
(6) Dieterich, D. *Prog. Org. Coat.* **1981**, *9*, 281−340.
(7) Sardon, H.; Engler, A.; Chan, J. M. W.; Coady, D.; O'Brien, J. M.; Mecerreyes, D.; Yang, Y.-Y.; Hedrick, J. *Green Chem.* **2013**, *15*, 1121−1126.
(8) Bayer, O. *Angew. Chem.* **1947**, *59*, 257−272.
(9) Wittbecker, E. L.; Katz, M. *J. Polym. Sci.* **1959**, *40*, 367−375.
(10) Silva, A. L.; Bordado, J. C. *Catal. Rev.: Sci. Eng.* **2004**, *46*, 31−51.
(11) Coady, D. J.; Horn, H. W.; Jones, G. O.; Sardon, H.; Engler, A. C.; Waymouth, R. M.; Rice, J. E.; Yang, Y. Y.; Hedrick, J. L. *ACS Macro Lett.* **2013**, *2*, 306−312.
(12) Sardon, H.; Irusta, L.; Fernández-Berridi, M. J. *Prog. Org. Coat.* **2009**, *66*, 291−295.
(13) Blank, W. J. *Macromol. Symp.* **2002**, *187*, 261−270.
(14) Blank, W. J.; He, Z. A.; Hessell, E. T. *Prog. Org. Coat.* **1999**, *35*, 19−29.
(15) Alsarraf, J.; Ammar, Y. A.; Robert, F.; Cloutet, E.; Cramail, H.; Landais, Y. *Macromolecules* **2012**, *45*, 2249−2256.
(16) Dechy-Cabaret, O.; Martin-Vaca, B.; Bourissou, D. *Chem. Rev.* **2004**, *104*, 6147−6176.
(17) Chuma, A.; Horn, H. W.; Swope, W. C.; Pratt, R. C.; Zhang, L.; Lohmeijer, B. G. G.; Wade, C. G.; Waymouth, R. M.; Hedrick, J. L.; Rice, J. E. *J. Am. Chem. Soc.* **2008**, *130*, 6749−6754.
(18) Pratt, R. C.; Lohmeijer, B. G. G.; Long, D. A.; Waymouth, R. M.; Hedrick, J. L. *J. Am. Chem. Soc.* **2006**, *128*, 4556−4557.
(19) Sanders, D. P.; Fukushima, K.; Coady, D. J.; Nelson, A.; Fujiwara, M.; Yasumoto, M.; Hedrick, J. L. *J. Am. Chem. Soc.* **2010**, *132*, 14724−14726.
(20) Mikami, K.; Lonnecker, A. T.; Gustafson, T. P.; Zinnel, N. F.; Pai, P.-J.; Russell, D. H.; Wooley, K. L. *J. Am. Chem. Soc.* **2013**, *135*, 6826−6829.
(21) Fèvre, M.; Pinaud, J.; Leteneur, A.; Gnanou, Y.; Vignolle, J.; Taton, D.; Miqueu, K.; Sotiropoulos, J.-M. *J. Am. Chem. Soc.* **2012**, *134*, 6776−6784.

(22) Makiguchi, K.; Ogasawara, Y.; Kikuchi, S.; Satoh, T.; Kakuchi, T. *Macromolecules* **2013**, *46*, 1772−1782.

(23) Kamber, N. E.; Jeong, W.; Waymouth, R. M.; Pratt, R. C.; Lohmeijer, B. G. G.; Hedrick, J. L. *Chem. Rev.* **2007**, *107*, 5813−5840.

(24) Dove, A. P. *ACS Macro Lett.* **2012**, *1*, 1409−1412.

(25) Kiesewetter, M. K.; Shin, E. J.; Hedrick, J. L.; Waymouth, R. M. *Macromolecules* **2010**, *43*, 2093−2107.

(26) Raynaud, J.; Absalon, C.; Gnanou, Y.; Taton, D. *J. Am. Chem. Soc.* **2009**, *131*, 3201−3209.

(27) Coutelier, O.; El Ezzi, M.; Destarac, M.; Bonnette, F.; Kato, T.; Baceiredo, A.; Sivasankarapillai, G.; Gnanou, Y.; Taton, D. *Polym. Chem.* **2012**, *3*, 605−608.

(28) Alsarraf, J.; Robert, F.; Cramail, H.; Landais, Y. *Polym. Chem.* **2013**, *4*, 904−907.

(29) Susperregui, N.; Delcroix, D.; Martin-Vaca, B.; Bourissou, D.; Maron, L. *J. Org. Chem.* **2010**, *75*, 6581−6587.

(30) Delebecq, E.; Pascault, J.-P.; Boutevin, B.; Ganachaud, F. *Chem. Rev.* **2012**, *113*, 80−118.

(31) Subrayan, R. P.; Zhang, S.; Jones, F. N.; Swarup, V.; Yezrielev, A. I. *J. Appl. Polym. Sci.* **2000**, *77*, 2212−2228.

(32) Nordstrom, D. J.; Stolarski, V. L. Proceedings of Waterborne, High-Solids, and Powder Coatings Symposium, February 5−7, 1997, New Orleans, LA; University of Southern Mississippi: Hattiesburg, MS, 1997.

(33) Odian, G. *Principles of Polymerization*; Wiley-Interscience John Wiley & Sons, Inc.: Hoboken, NJ, 2004.

(34) Schmidt, M. W.; Baldridge, K. K.; Boatz, J. A.; Elbert, S. T.; Gordon, M. S.; Jensen, J. H.; Koseki, S.; Matsunaga, N.; Nguyen, K. A.; Su, S.; Windus, T. L.; Dupuis, M.; Montgomery, J. A. *J. Comput. Chem.* **1993**, *14*, 1347−1363.

(35) Peverati, R.; Truhlar, D. G. *J. Phys. Chem. Lett.* **2011**, *2*, 2810−2817.

(36) Geometry optimizations were performed with the 6-311+G(2d,p) basis set. Followed by single point energy calculations with the aug-cc-pVTZ basis set. The 6-311+G(2d,p) basis set over the more economical 6-31+G(d) was chosen as an initial survey using the latter showed significant BSSE effects for acids containing sulfur and/or fluorine atoms. A detailed description about the computational protocol used in this study is included in the Supporting Information.

(37) Ditchfield, R.; Hehre, W. J.; Pople, J. A. *J. Chem. Phys.* **1971**, *54*, 724−728.

(38) Hehre, W. J.; Ditchfield, R.; Pople, J. A. *J. Chem. Phys.* **1972**, *56*, 2257−2261.

(39) Devendra, R.; Edmonds, N. R.; Söhnel, T. *J. Mol. Catal. A: Chem.* **2013**, *366*, 126−139.

(40) Sardon, H.; Irusta, L.; Fernández-Berridi, M. J.; Lansalot, M.; Bourgeat-Lami, E. *Polymer* **2010**, *51*, 5051−5057.

16241

dx.doi.org/10.1021/ja408641g | *J. Am. Chem. Soc.* 2013, 135, 16235−16241